

# Niobium oxide acidity studied by proton broad-line NMR at 4 K and MAS NMR at room temperature

Patrice Batamack, Robert Vincent and Jacques Fraissard

*Laboratoire de Chimie des Surfaces associé au CNRS, URA 1428, Université Pierre et Marie Curie, Tour 55, 4 Place Jussieu, 75252 Paris Cedex 05, France*

Received 5 August 1995; accepted 20 September 1995

The quantitative study of the Brønsted acidity of niobic acid ( $\text{Nb}_2\text{O}_5 \cdot x\text{H}_2\text{O}$ ) using broad-line  $^1\text{H}$  NMR at 4 K has been performed by interacting niobic acid, pretreated at 573 K under vacuum, with water molecules. The number of oxyprotonated species ( $\text{H}_3\text{O}^+$ , and  $\text{H}_2\text{O} \cdots \text{HO}$  species formed, unreacted acidic OH groups or excess  $\text{H}_2\text{O}$  molecules) deduced from the simulations of the broad-line  $^1\text{H}$  NMR spectra shows a continuous increase in the number of  $\text{H}_3\text{O}^+$  species with adsorbed water molecules. This increase may be due to a classical dilution effect or to a synergistic interaction between Brønsted and Lewis acid sites. These results are compared with those of some HY zeolites with or without framework defects.

**Keywords:** niobic acid; acidity;  $^1\text{H}$  broad-line NMR;  $^1\text{H}$  MAS NMR

## 1. Introduction

The diverse applications of niobic acid [1] and its marked ability, when treated at relatively low temperatures ( $423 \leq T_t \leq 573$  K), to catalyze various reactions in which strong acid sites are required and water molecules are involved makes it a particularly interesting compound. Dehydration [2], esterification [3], hydration [4], hydrolysis [5], isomerization and polymerization [2], etc., are among the reactions catalyzed by niobic acid.

Sen et al. [6, 7] have investigated the nature and structure of niobic acid. They conclude that niobic acid treated at 423 K is an isopolyacid, and from analytical results it can be written as  $\text{H}_8\text{Nb}_6\text{O}_{19}$ . According to broad-line  $^1\text{H}$  NMR quantitative analysis in the range of  $573 \leq T_t \leq 1273$  K the polymeric niobium oxide contains two hydroxide groups per three  $\text{Nb}_2\text{O}_5$  molecules in the form of hydroxyl groups attached to Nb atoms. These authors state that the basic unit of this polymeric form can be represented as  $\text{H}_2\text{Nb}_6\text{O}_{16}$ . DTA and TG analysis show that niobium pentaoxide hydrate is completely dehydrated by heating to 573 K [2].

The surface acidity of niobic acid was studied by *n*-butylamine titration using Hammett indicators, infrared spectroscopy of the adsorbed pyridine [2, 8] and by volumetric and gravimetric analysis of adsorbed  $\text{NH}_3$  [9]. The surface of  $\text{Nb}_2\text{O}_5 \cdot x\text{H}_2\text{O}$  contains both Lewis and Brønsted acid sites [2, 10]. The authors show that for niobic acid treated at  $373 \leq T_t \leq 573$  K there is a large number of acid sites having an acidity strength of  $H_0 = -5.6$ . Infrared spectroscopy of the adsorbed pyridine reveals that the pyridinium ion band intensity at  $1540\text{ cm}^{-1}$  is greatest at  $T_t = 373$  K. At  $T_t = 573$  K, this band has almost disappeared while the bands of pyridine coordinately bonded to the surface, at 1610, 1480 and

$1440\text{ cm}^{-1}$ , are still present. The coordinately bonded pyridine band ( $1446\text{--}1448\text{ cm}^{-1}$ ) intensity is strongest for niobic acid activated at 573 K. Niobic acid calcined at  $773 \leq T_t \leq 873$  K is almost catalytically inactive although the  $^1\text{H}$  NMR quantitative analysis claimed that niobium oxide still contains two hydroxyl groups at  $T_t \leq 1273$  K [6].

The surface acidity of niobium oxide depends on the preparation method and conditions [11]. Ushikubo et al. have studied the factors affecting the acid strength of niobic acid and have been able to prepare niobic acid with an acid strength of  $H_0 = -8.2$ . Sulfation and phosphorylation resulted in a significant increase of the acidity of niobium oxide [8, 9]. Recently, Guo and Qian [12] showed that crystallized niobic acid possesses more acid sites with higher strength than uncrystallized, sulfated or phosphorylated niobic acid.

Broad-line  $^1\text{H}$  NMR at 4 K is a relatively recent method of investigating the surface acidity of solids using water molecules as a base. The method, which has been successfully applied to many acidic solids [13–19] leads to a direct quantification of the  $\text{H}_3\text{O}^+$  species when they are formed and of the number of  $\text{H}_2\text{O} \cdots \text{HO}$  species for weaker solid surface Brønsted sites.

Since niobic acid showed a good catalytic activity for reactions in which water molecules are involved, the compound is a suitable candidate to our  $^1\text{H}$  NMR surface acidity studies using water as base.

## 2. Experimental

Niobium pentaoxide hydrate  $\text{Nb}_2\text{O}_5 \cdot x\text{H}_2\text{O}$  (niobia HY-340 AD/1123) from CBMM Laboratory, Brazil, is provided by Nissho Iwai Corporation, Japan. The sur-

face area of the sample treated at  $T_t = 573$  K measured by nitrogen adsorption at 77 K is  $158 \text{ m}^2 \text{ g}^{-1}$ . About 0.6 g of sample in a glass ampule are evacuated at room temperature to  $10^{-2}$  Pa, then heated at a rate of  $24 \text{ K h}^{-1}$  up to 573 K for at least 2 h. The amount of desorbed water is about 19% by weight. The number of protons on this calcined sample is determined from the  $^1\text{H}$  NMR MAS spectrum by measuring the area under the curve including the sidebands and using distilled water as the absolute reference. Water vapour is introduced at a constant temperature of 300 K in several steps, at pressures much lower than saturation; the amount of water is determined gravimetrically. The sample is held at 383 K overnight to ensure homogeneous distribution of the adsorbed water molecules and then sealed in thin 5 mm o.d. glass ampules.

$^1\text{H}$  MAS NMR experiments at room temperature are performed on a Bruker MSL-400 spectrometer with a home-made 5 mm probe. The rotation frequency of sealed tubes is 3500–4500 Hz. The weak residual signal of the probe is subtracted from the total signal. Chemical shifts are expressed with respect to liquid TMS as external reference using the usual conventions.

The broad-line  $^1\text{H}$  NMR spectra are recorded at 4 K on a home-made continuous wave 60 MHz spectrometer with phase detection and signal accumulation. The weak probe signal is subtracted from each spectrum. The recorded signal is the derivative,  $dF(h)/dh$ , of the absorption signal,  $F(h)$ , in which  $h$  represents the variation of the applied magnetic field relative to the center of the spectrum. They are theoretically symmetrical with respect to the centre and, in practice, the two parts of each experimental spectrum are averaged; for this reason we show only half of each spectrum.

The simulated spectra of broad-line  $^1\text{H}$  NMR spectra correspond to the weighted sum of the oxyprotonated species involved and for which magnetic configurations are calculated [13,20–24]. (i)  $\text{H}_2\text{O}$ , a  $r$ -distant two-spin configuration; (ii)  $\text{H}_3\text{O}^+$ , a magnetic configuration with three  $r$ -distant spins at the vertices of an equilateral triangle; (iii)  $\text{H}_2\text{O} \cdots \text{HO}$  or distorted  $\text{H}_3\text{O}^+$ , a magnetic configuration with three spins at the vertices of an isosceles triangle, where  $r$  is the base and  $r'$  the equal sides; (iv) OH, a two-spin configuration or a pure Gaussian and/or a pure Lorentzian function. Each of the corresponding functions (except the Gaussian and the Lorentzian functions) is convoluted by a Gaussian which takes into account the interaction between the protons of the configuration and those belonging to neighboring configurations and also those of the nuclei with non-zero spin in the environment ( $^{93}\text{Nb}$  in the present case). When the effect of these non-zero spins is small the parameter of each Gaussian is related to a distance  $X$  which, in the case of two adjacent magnetic configurations, expresses the mean interaction of protons in terms of the distance between these two configurations. For a distribution of magnetic configurations at the surface,  $X$  expresses the

mean interaction between a given configuration and its nearest environment. The broadening parameter,  $X$ , is determined by the simulation. The calculations are referred to the unit block  $\text{H}_2\text{Nb}_6\text{O}_{16}$  and the numerical base takes into account the total number of protons in the sample, which is equal to the number of hydroxyl groups plus twice the number of water molecules introduced. Moreover, we applied some constraints since the number of independent parameters for each simulation is high. We impose the condition that the water molecules introduced do not dissociate to produce additional OH groups. Finally, the distances  $r$  found must lie in the range corresponding to the various oxygen–proton species identified, which is always the case, and for each configuration the value of  $X$  must be greater than (or at least equal to) that of  $r$  and  $r'$ .

### 3. Results

#### 3.1. $^1\text{H}$ MAS NMR

The  $^1\text{H}$  MAS NMR spectra are depicted in fig. 1. The spectrum of the anhydrous sample (fig. 1a) presents two signals, one at 2.9 ppm, 1120 Hz wide at half-height, and a small, broad shoulder at around 8 ppm with strong sidebands. The number of protons per gram of this sample is  $1.6 \times 10^{21}$ . When 0.27 water molecules per  $\text{H}_2\text{Nb}_6\text{O}_{16}$  unit are added, the spectrum shows two signals (fig. 1b): a very weak signal at 1.5 ppm and a Lorentzian signal 1.4 kHz wide at 5.7 ppm with strong spinning sidebands. In the presence of one water molecule per  $\text{H}_2\text{Nb}_6\text{O}_{16}$  unit, the 1.5 ppm peak becomes almost invisible and a 4.6 kHz wide signal is observed at 6.4 ppm (fig. 1c). The chemical shift of this line decreases upon addition of 2.3  $\text{H}_2\text{O}$  or more per  $\text{H}_2\text{Nb}_6\text{O}_{16}$  unit and the spinning sidebands are significantly weakened; the weak signal at 1.5 ppm is no longer visible (fig. 1d). The remaining single signal remains Lorentzian for  $\text{H}_2\text{Nb}_6\text{O}_{16} \cdot 2.3\text{H}_2\text{O}$  sample and less and less wide for samples containing more water molecules (figs. 1e–1f). The chemical shift of the exchanged signal on the fully hydrated sample ( $\text{H}_2\text{Nb}_6\text{O}_{16} \cdot 10.6\text{H}_2\text{O}$ ) is 5.1 ppm.

#### 3.2. $^1\text{H}$ broad-line NMR at 4 K

Fig. 2 shows the evolution of some 4 K broad-line  $^1\text{H}$  NMR spectra with increasing water concentration  $\text{H}_2\text{Nb}_6\text{O}_{16} \cdot 0.54\text{H}_2\text{O}$ ,  $\text{H}_2\text{Nb}_6\text{O}_{16} \cdot 2.3\text{H}_2\text{O}$ , and  $\text{H}_2\text{Nb}_6\text{O}_{16} \cdot 4.8\text{H}_2\text{O}$ . In each case, it was possible to simulate the experimental spectrum. The shape of the spectrum depends significantly on the sample water content. The spectrum of the anhydrous sample is poorly resolved and the fit is achieved with a two-spin line describing the magnetic interaction of the hydroxyl groups of the sample. All the other spectra consist of three maxima (at about 1.7, 6, and  $(10.5\text{--}11) \times 10^{-4}$  T) well resolved for

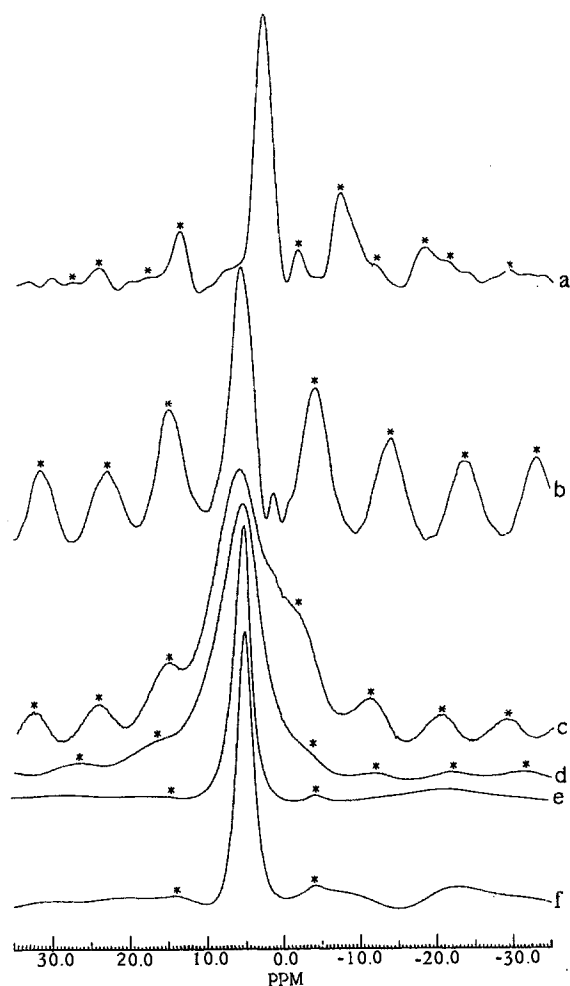


Fig. 1.  $^1\text{H}$  MAS NMR spectra of niobium oxide samples: non-loaded niobium oxide (a);  $\text{H}_2\text{Nb}_6\text{O}_{16}\cdot 0.27\text{H}_2\text{O}$  (b);  $\text{H}_2\text{Nb}_6\text{O}_{16}\cdot 1.06\text{H}_2\text{O}$  (c);  $\text{H}_2\text{Nb}_6\text{O}_{16}\cdot 2.3\text{H}_2\text{O}$  (d);  $\text{H}_2\text{Nb}_6\text{O}_{16}\cdot 4.8\text{H}_2\text{O}$  (e);  $\text{H}_2\text{Nb}_6\text{O}_{16}\cdot 10.6\text{H}_2\text{O}$  (f). Asterisks denote spinning sidebands.

low water loading. The simulated spectrum of the  $\text{H}_2\text{Nb}_6\text{O}_{16}\cdot 0.54\text{H}_2\text{O}$  sample reveals three species:  $\text{H}_3\text{O}^+$  species,  $\text{H}_2\text{O}\cdots\text{HO}$  and OH groups. For the hydroxyl groups two different curves are required to obtain an acceptable fit, two-spin and Gaussian lines (fig. 2a). But for the  $\text{H}_2\text{Nb}_6\text{O}_{16}\cdot 1.06\text{H}_2\text{O}$  sample, besides the signals characterizing the hydronium ions and the hydrogen-bonded species, a single Gaussian line allows the correct simulation of the experimental spectrum. When the number of water molecules is greater than or equal to 2.3  $\text{H}_2\text{O}$  per  $\text{H}_2\text{Nb}_6\text{O}_{16}$  (figs. 2b and 2c) all the spectra contain water molecules as well as  $\text{H}_3\text{O}^+$  and  $\text{H}_2\text{O}\cdots\text{HO}$  species. No hydroxyl group without interaction is observed for these water loadings. Table 1 summarizes the concentrations of the different oxyprotonated species obtained for each sample and given in table 2 are the distance parameters used to simulate of the spectra.

#### 4. Discussion

The number of protons per gram of sample treated

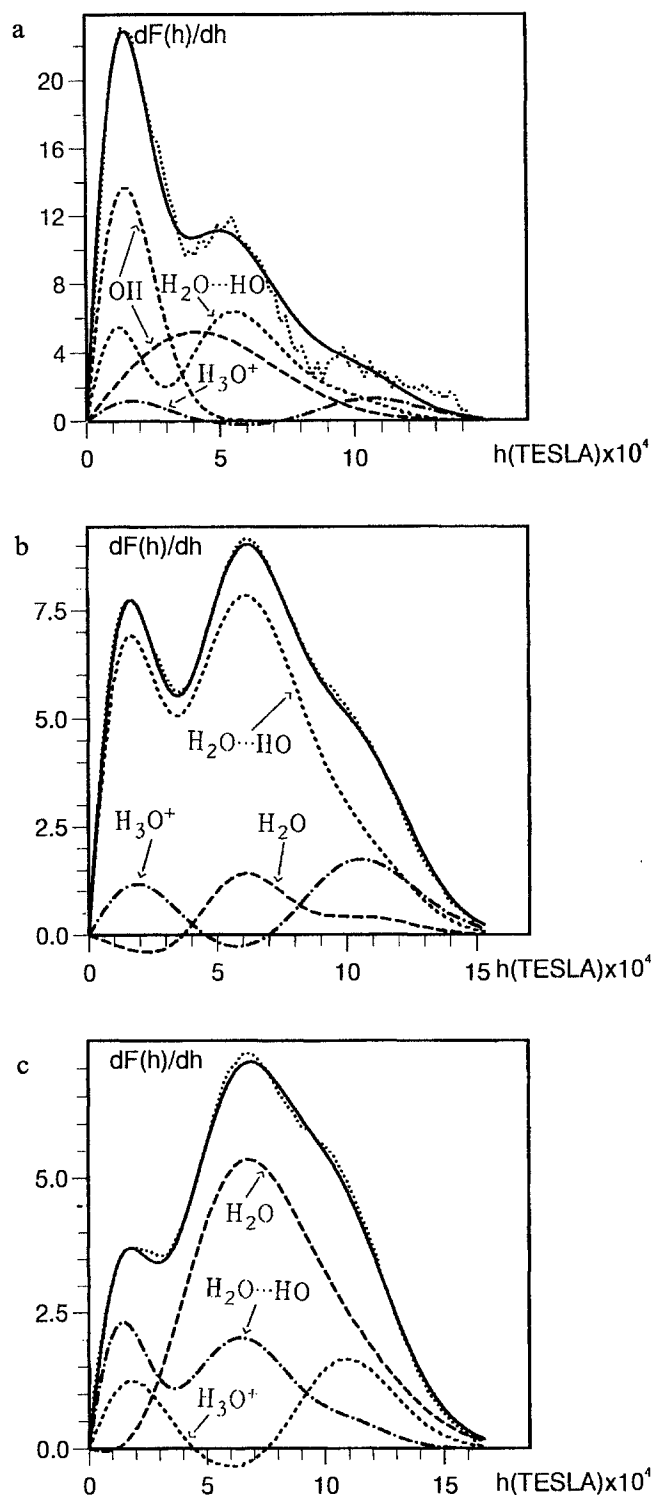


Fig. 2. Half derivative  $^1\text{H}$  NMR broad-line spectra for niobium oxide samples:  $\text{H}_2\text{Nb}_6\text{O}_{16}\cdot 0.54\text{H}_2\text{O}$  (a);  $\text{H}_2\text{Nb}_6\text{O}_{16}\cdot 2.3\text{H}_2\text{O}$  (b);  $\text{H}_2\text{Nb}_6\text{O}_{16}\cdot 7.6\text{H}_2\text{O}$  (c). The weighted contribution of each oxygen-protonated species is shown on the spectrum. (···) Experimental and (---) fitted spectra.

at 573 K is  $1.6 \times 10^{+21}$ . By comparing this number with the theoretical number of protons per gram of  $\text{H}_2\text{Nb}_6\text{O}_{16}$ ,  $1.5 \times 10^{+21}$ , we concluded that niobic acid evacuated at 573 K contains two hydroxyl groups, confirming the results of ref. [6].  $^1\text{H}$  MAS NMR shows the

Table 1

Number of oxygen-protonated species per  $\text{H}_2\text{Nb}_6\text{O}_{16}$  unit after adsorption of the number of water molecules per  $\text{H}_2\text{Nb}_6\text{O}_{16}$  unit

No. of adsorbed water molecules	No. of $\text{H}_3\text{O}^+$ ions	No. of $\text{H}_2\text{O} \cdots \text{HO}$ groups	No. of "free" acidic OH groups	No. of water molecules
0.0	0.0	0.0	$2.00 \pm 0.20$	0.0
$0.54 \pm 0.05$	$0.13 \pm 0.02$	$0.43 \pm 0.05$	$1.45 \pm 0.16$	0.0
$1.06 \pm 0.05$	$0.23 \pm 0.03$	$0.82 \pm 0.09$	$0.95 \pm 0.09$	0.0
$2.3 \pm 0.1$	$0.39 \pm 0.05$	$1.57 \pm 0.17$	0.0	$0.33 \pm 0.04$
$3.8 \pm 0.2$	$0.58 \pm 0.07$	$1.47 \pm 0.15$	0.0	$1.7 \pm 0.2$
$4.8 \pm 0.2$	$0.83 \pm 0.09$	$1.18 \pm 0.12$	0.0	$2.8 \pm 0.3$
$7.6 \pm 0.3$	$0.94 \pm 0.09$	$1.06 \pm 0.11$	0.0	$5.6 \pm 0.5$
$10.6 \pm 0.5$	$1.00 \pm 0.10$	$1.00 \pm 0.10$	0.0	$8.6 \pm 0.8$

interaction between hydroxyl groups and water molecules after adsorption of a small amount of water. The signal observed between 5.1 and 6.4 ppm is due to fast chemical exchange between the protons of  $\text{H}_3\text{O}^+$  ions,  $\text{H}_2\text{O} \cdots \text{HO}$ , residual OH groups and water molecules at room temperature. High resolution proton  $^1\text{H}$  MAS NMR at room temperature is always subject to chemical exchange between species. At low water loadings, when the number of water molecules introduced is less than the number of acidic OH groups, a signal at 1.5 ppm arises. This signal is masked by that of the acidic hydroxyl groups on the non-loaded sample and may be due to impurities in the sample. These hydroxyl groups represent about 4% of the total number of protons in the  $\text{H}_2\text{Nb}_6\text{O}_{16} \cdot 0.27\text{H}_2\text{O}$  sample. The number of  $\text{H}_3\text{O}^+$  ions per acid site increases continuously with the number of adsorbed water molecules (fig. 3). Up to 2.4  $\text{H}_2\text{O}$  per acid site, the slope of the curve is high and decreases above this value. This gradual increase of the ionization coefficient may be due to dilution by the addition of water molecules. In fact, it is well known that in aqueous solution the dilution of weak and medium electrolytes increases the ionization coefficient. Although aqueous solution conditions are not achieved in our experiments, the open surface of niobium oxide may favour the interaction of water molecules and the hydrogen-bonded species. Ben et al. [7] showed that water molecules are attached to the peripheral oxygen atoms of niobic acid through hydrogen bonding. The results of the simulation

of the broad-line spectra (table 1) show that the number of hydrogen-bonded species decreases while that of hydronium ions rises when the water molecules concentration is increased. Furthermore, in table 2 the distance parameter,  $X$ , of water molecules diminishes by increasing the water content of the sample proving the proximity of these molecules to the others. Let us recall that  $X$  is the average shortest distance between protons and/or other nuclei of distinct magnetic configurations. In contrast, our studies of an HY zeolite ( $\text{Si}/\text{Al} = 2.4$ ) without defects show that, when the ratio of the number of water molecules to the number of acidic OH groups,  $R_n$ , exceeds unity, the ionization coefficient remains almost constant [19]. The large cavities and the channels of the zeolite do not favour the dilution effect. Water molecules seem to occupy preferentially the empty space of the zeolite instead of getting close to the hydrogen-bonded species. However, in the case of an HY zeolite ( $\text{Si}/\text{Al} = 4.4$ ), presenting Lewis acid sites after partial dealumination by an aqueous solution of  $(\text{NH}_4)_2\text{SiF}_6$ , the ionization coefficient is constant for  $1 \leq R_n \leq 2$  and increases when  $R_n \geq 2$  [25,26]. In the case of zeolites we attributed this to synergy between Lewis sites Al atoms and Brønsted sites through the network of hydrogen bonds established by water molecules and connecting all acid sites when  $R_n \geq 2$  [27]. The surface acidity of hydrated niobium pentaoxide treated at 573 K consists mainly of Lewis acid sites [2]. Consequently, the continuous increase of the number of  $\text{H}_3\text{O}^+$  ions when  $R_n \geq 1$

Table 2

Distance parameters (in pm) used for simulations of  $\text{H}_2\text{Nb}_6\text{O}_{16} \cdot x\text{H}_2\text{O}$  spectra

No. of adsorbed water molecules per $\text{H}_2\text{Nb}_6\text{O}_{16}$ unit	Hydroxonium ions (isosceles symmetry)			$\text{H}_2\text{O} \cdots \text{HO}$ groups			Acidic OH groups		$\text{H}_2\text{O}$ molecules	
	$r \pm 2$	$r' \pm 5$	$X \pm 5$	$r \pm 2$	$r' \pm 5$	$X \pm 5$	$r \pm 2$	$X \pm 5$	$r \pm 2$	$X \pm 5$
$0.54 \pm 0.05$	162	167	218	164	258	265	195	195		
							Gaussian	244		
							192	192		
$1.06 \pm 0.05$	161	169	223	158	224	253				
$2.3 \pm 0.1$	158	169	216	158	229	233			157	233
$3.8 \pm 0.2$	158	169	216	158	229	233			157	204
$4.8 \pm 0.2$	157	168	215	158	231	236			157	204
$7.6 \pm 0.3$	156	167	220	157	229	240			158	198
$10.6 \pm 0.5$	157	168	219	157	232	243			158	197

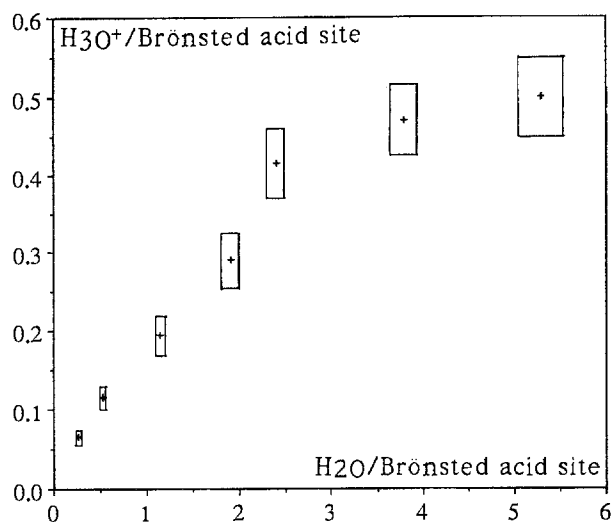


Fig. 3. Variation of  $\text{H}_3\text{O}^+$  concentration with adsorbed  $\text{H}_2\text{O}$  per Brønsted acid site.

could also be accounted for by synergy between Lewis site Nb atoms and Brønsted sites.

The symmetry of  $\text{H}_3\text{O}^+$  ions is not optimal. The best fits are obtained using a magnetic configuration with protons at the apices of an isosceles triangle for the hydroxonium ions (see table 2) (the lowest symmetry then programmed). When the number of adsorbed water molecules per acid site is 1.0, the dissociation coefficient is 0.2, as for HY zeolites ( $\text{Si}/\text{Al} = 2.4$ ) [19]. Although the number of acid sites is very low on the surface of niobic acid compared to that of zeolites HY, the acid strength of these compounds is similar. The number of hydroxonium ions per acid site reaches 0.5 for the fully hydrated sample,  $\text{H}_2\text{Nb}_6\text{O}_{16} \cdot 10.6\text{H}_2\text{O}$  (see table 1). 50% of acidic OH groups form  $\text{H}_3\text{O}^+$  ions; the other 50% lead to the hydrogen-bonded species. At saturation, a plateau is observed. Thus, the two hydroxyl groups of niobic acid do not have the same strength; one is stronger than the other.

## 5. Conclusion

Study of the surface acidity of the hydrated niobium pentaoxide treated at 573 K using  $^1\text{H}$  MAS NMR at room temperature and broad-line NMR at 4 K shows that the number of hydroxyl groups on the anhydrous sample is low (2 H atoms per  $[\text{Nb}_6\text{O}_{16}]^{2-}$ ). According to the simulation of the broad-line  $^1\text{H}$  NMR spectra the number of hydronium ions increases continuously to reach 0.5 per acid site for  $\text{H}_2\text{Nb}_6\text{O}_{16} \cdot 10.6\text{H}_2\text{O}$  (full hydration). The increase of the ionization coefficient may be explained by the dilution effect and/or the synergy between Lewis acid Nb atoms and Brønsted sites. At full hydration, 50% of the acid sites are ionized revealing that of the two acid sites of niobium oxide only one is particularly strong. When the ratio of the number of water molecules adsorbed to the number of hydroxyl

groups of the sample,  $R_n$ , is unity, the ionization coefficient of niobic acid deduced of this study, 0.2, is the same as that of an HY zeolite ( $\text{Si}/\text{Al} = 2.4$ ) without defects. This value expresses the fact that the mean surface acidity of these compounds is similar. In contrast to the continuous increase of the hydronium ion concentration with water molecules in niobium oxide, a plateau is observed for HY zeolite ( $\text{Si}/\text{Al} = 2.4$ ) without defects when  $R_n$  is greater than or equal to unity. In contrast, for HY zeolite ( $\text{Si}/\text{Al} = 4.4$ ) with framework defects, partially dealuminated by a solution of  $(\text{NH}_4)_2\text{SiF}_6$  and containing Lewis acid sites, the concentration of  $\text{H}_3\text{O}^+$  ions increases for  $R_n \geq 2$ . The surface of niobium oxide and the presence of Lewis site Nb atoms seem to favour the dissociation of the acidic hydroxyl groups of this compound.

## Acknowledgement

We are grateful to the CBMM Laboratory of Brazil and the Nissho Iwai Corporation of Japan for providing us with the hydrated pentaoxide sample and to Professor Kozo Tanabe for his great help and encouragement.

## References

- [1] K. Tanabe, *Catal. Today* 8 (1990) 1.
- [2] T. Iizuka, K. Ogasawara and K. Tanabe, *Bull. Chem. Soc. Jpn.* 56 (1983) 2927.
- [3] Z. Chen, T. Iizuka and K. Tanabe, *Chem. Lett.* (1984) 1085.
- [4] K. Ogasawara, T. Iizuka and K. Tanabe, *Chem. Lett.* (1984) 645.
- [5] T. Iizuka, S. Fujie, T. Ushikubo, Z. Chen and K. Tanabe, *Appl. Catal.* 28 (1986) 1.
- [6] B.K. Sen, A.V. Saha and N. Chatterjee, *Mater. Res. Bull.* 16 (1981) 923.
- [7] B.K. Sen and A.V. Saha, *Mater. Res. Bull.* 17 (1982) 161.
- [8] S. Okazaki, M. Kurimata, T. Iizuka and K. Tanabe, *Bull. Chem. Soc. Jpn.* 60 (1987) 37.
- [9] A. Kurosaki, T. Okuyama and S. Okazaki, *Bull. Chem. Soc. Jpn.* 60 (1987) 3541.
- [10] K. Tanabe, M. Misono, Y. Ono and H. Hattori, in: *New Solid Acids and Bases*, Stud. Surf. Sci. Catal., Vol. 51 (Elsevier, Amsterdam, 1989) p. 61.
- [11] T. Ushikubo, T. Iizuka, H. Hattori and K. Tanabe, *Catal. Today* 16 (1993) 291.
- [12] C. Guo and Z. Qian, *Catal. Today* 16 (1993) 379.
- [13] C. Dorémieux-Morin, *J. Magn. Reson.* 21 (1976) 419.
- [14] C. Dorémieux-Morin, *J. Magn. Reson.* 33 (1979) 505.
- [15] H. Arribat, Y. Piffard and C. Dorémieux-Morin, *Solid State Ionics* 7 (1982) 91.
- [16] C. Dorémieux-Morin, M.A. Enriquez, J. Sanz and J. Fraissard, *J. Colloid Interf. Sci.* 95 (1983) 502.
- [17] P. Batamack, C. Dorémieux-Morin, R. Vincent and J. Fraissard, *Chem. Phys. Lett.* 180 (1991) 545.
- [18] P. Batamack, C. Dorémieux-Morin, J. Fraissard and D. Freude, *J. Phys. Chem.* 95 (1991) 3790.
- [19] P. Batamack, C. Dorémieux-Morin, R. Vincent and J. Fraissard, *J. Phys. Chem.* 97 (1993) 9779, and references therein.
- [20] G.E. Pake, *J. Phys. Chem.* 16 (1948) 327.

- [21] E.R. Andrew and N.D. Finch, *Proc. Phys. Soc.* 70B (1957) 980.
- [22] E.R. Andrew and R.J. Bersolin, *J. Phys. Chem.* 18 (1950) 159.
- [23] R.E. Richards and Smith, *JAS Trans. Faraday Soc.* 48 (1952) 675.
- [24] A.L. Porte, H.S. Gutowsky and J.E. Boggs, *J. Phys. Chem.* 36 (1962) 1695.
- [25] P. Batamack, C. Dorémieux-Morin and J. Fraissard, *Catal. Lett.* 11 (1991) 119.
- [26] P. Batamack, C. Dorémieux-Morin and J. Fraissard, *Proc. 10th Int. Congress on Catalysis*, Budapest, 1992, eds. J. Guzzi, F. Solymosi and P. Tétényi (Elsevier, Amsterdam, 1993) p. 243.
- [27] P. Batamack, C. Dorémieux-Morin, R. Vincent and J. Fraissard, *Microporous Mater.* 2 (1994) 515.